

Regioselective Substitution at the 1,3- and 6,8-Positions of Pyrene for the Construction of Small Dipolar Molecules

Xing Feng,^{†,‡} Hirotugu Tomiyasu,[‡] Jian-Yong Hu,^{*,§} Xianfu Wei,[†] Carl Redshaw,^{||} Mark R. J. Elsegood,[⊥] Lynne Horsburgh,[⊥] Simon J. Teat,[#] and Takehiko Yamato^{*,‡}

[†]Beijing Institute of Graphic Communication, Beijing 102600, P. R. China

[‡]Department of Applied Chemistry, Faculty of Science and Engineering, Saga University, Honjo-machi 1, Saga 840-8502, Japan

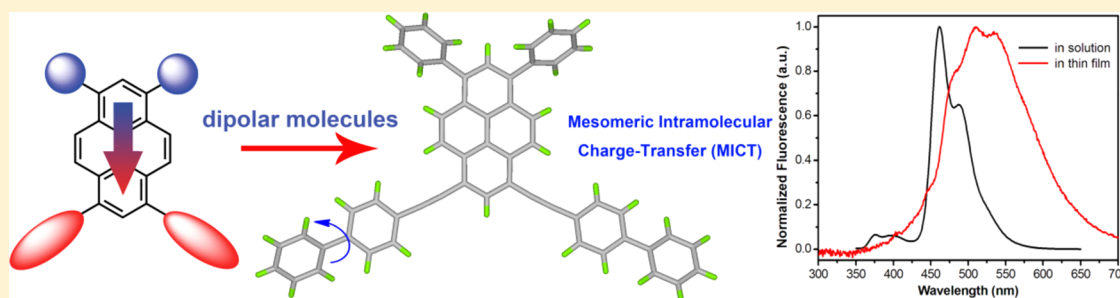
[§]School of Materials Science and Engineering, Shannxi Normal University, Xi'an, 710062 Shannxi, P. R. China

^{||}Department of Chemistry, The University of Hull, Cottingham Road, Hull, Yorkshire HU6 7RX, U.K.

[⊥]Chemistry Department, Loughborough University, Loughborough, Leicestershire LE11 3TU, U.K.

[#]Advanced Light Source, Berkeley National Laboratory, 1 Cyclotron Road, Berkeley, California 94720, United States

S Supporting Information



ABSTRACT: This article presents a novel asymmetrical functionalization strategy for the construction of dipolar molecules via efficient regioselective functionalization along the Z-axis of pyrene at both the 1,3- and 6,8-positions. Three asymmetrically substituted 1,3-diphenyl-6,8-R-disubstituted pyrenes were fully characterized by X-ray crystallography, photophysical properties, electrochemistry, and density functional theory calculations.

INTRODUCTION

The construction of dipolar molecules with donor–acceptor (D–A) type structures are of interest given their potential application in organic optoelectronic devices.¹ Such dipolar architectures can, via a suitable choice of the D–A units, fine-tune the electron redistribution, facilitate simultaneous manipulation of the HOMO–LUMO energy gap and the emission color by intramolecular charge transfer (ICT),² control crystallinity,³ and be used to self-assemble molecular morphologies.⁴

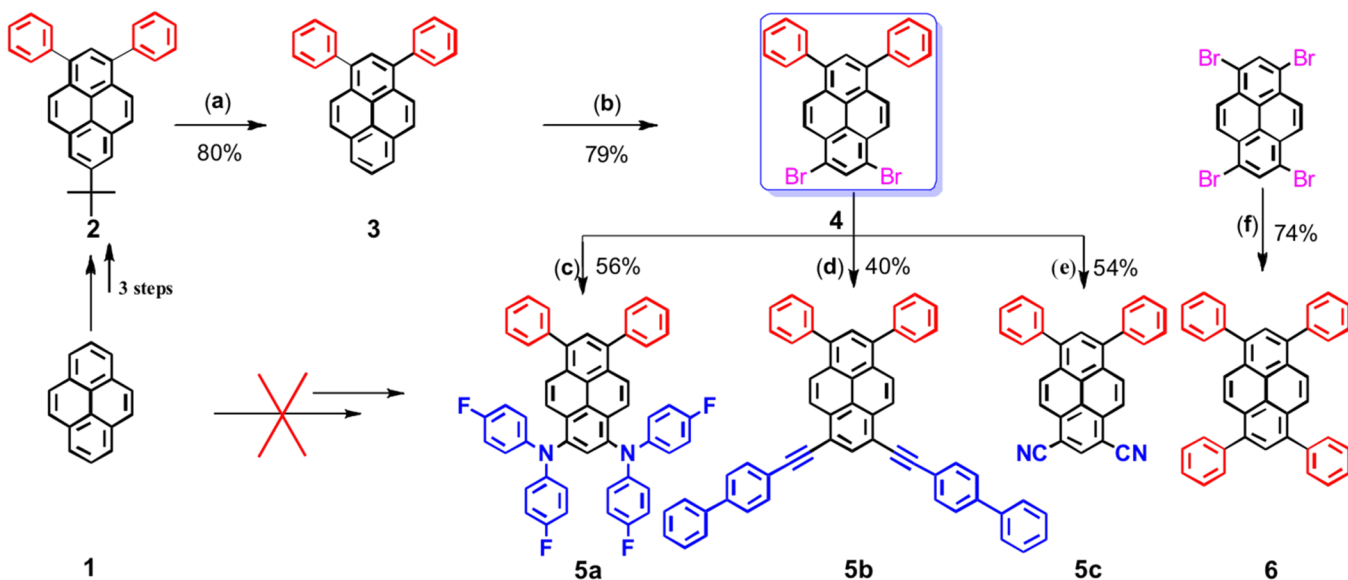
Pyrene⁵ belongs to a family of polycyclic aromatic hydrocarbons (PAHs) with a natural electron-donating role and an electron-accepting role.⁶ Apart from other PAHs like anthracene⁷ and fluorene,⁸ pyrene that possess the equivalent activity of the sites at the 1-, 3-, 6-, and 8-positions, it is different challenge to develop an effectively rational synthetic strategy for the asymmetric functionalization of pyrene. Typically, tetrabromopyrene and pyrene tetraone derivatives as key precursors were extensively utilized in the construction of PAHs for semiconductor applications, via the introduction of terminal moieties.^{5,9} Until now, few examples of pyrene chemistry have focused on constructing a “push–pull” system or investigating the effect of the electron-donating and

-accepting strength on the emission color of dipolar molecules, or the regio-chemical relationship between donor and acceptor units.

Recently, the Kim group and the Lee group developed a set of tetrakis-substituted pyrenes functionalized with electron donor and electron acceptor moieties located at the 1,6- and 3,8-positions randomly in nature, respectively.¹⁰ However, reports focusing on regioselectively substituted pyrene derivatives for bipolar materials are scant, because of the lack of straightforward strategies for modifying the pyrene core. Müllen et al. reported the selective asymmetric functionalization of pyrene at the K-region for use in organic field-effect transistors via a two-step chemical functionalization.¹¹ Meanwhile, Bodwell et al. reported a regioselective synthesis of 4,5-dialkoxy-1,8-dibromopyrenes for preparing 1,8-pyrenylene-ethynylene macrocycles.¹² After that, a series pyrene derivatives with D–A substituents of the pyrene derivative in the K-region was presented as follows.¹³ Very recently, both strong donors and acceptors were introduced into the K-region and the 2,7-positions, respectively, via 2,7-dibromo- and 2,7-diiodopyrene-

Received: September 10, 2015

Published: October 5, 2015

Scheme 1. Synthetic Route for the Preparation of 5 and 6^a

^a(a) Nafion-H, *o*-xylene, 160 °C, 24 h; (b) BTMABr₃ (benzyltrimethylammonium tribromide), CH₂Cl₂/MeOH, rt, 12 h; (c) NHPPh₂F, Pd(OAc)₂/(*t*Bu)₃P/K₂CO₃, toluene, 100 °C, 24 h; (d) 4-ethynyl-1,1'-biphenyl, [PdCl₂(PPh₃)₂], CuI, PPh₃, Et₃N/DMF (1:1), 48 h, 100 °C; (e) CuCN, NMP, 48 h, 180 °C; (f) phenylboronic acid, Pd(PPh₃)₄, K₂CO₃, toluene, 90 °C, 24 h.

4,5,9,10-tetraones as the key intermediates.¹⁴ Such novel synthetic procedures at the pyrene core not only greatly enrich our knowledge of synthetic chemistry but also stimulate further research into semiconductor materials.

Unlike the previously mentioned studies, our interest stems from exploring new effective strategies for preparing asymmetrically substituted pyrene along the *Z*-axis to be used in high-performance electroluminescence material applications. Previously, we have released a novel approach for modifying both at active position of 1,3- and *K*-region of 4,5,9,10-position using classical methods from 1,3-dibromo-7-*tert*-butylpyrene in considerable yield;¹⁵ in this case, a *tert*-butyl group plays a role in protecting the ring against electrophilic attack at the 6- and 8-positions.¹⁶ Herein, we further present a novel synthetic strategy for realizing regioselective substitution at the 1,3- and 6,8-positions of pyrene for the construction of dipolar molecules.

RESULTS AND DISCUSSION

Assuming that the *tert*-butyl group can be removed by an effective approach, the effective approach to regioselective substitution at the 1,3- and 6,8-positions of pyrene would be achievable. On the basis of our knowledge, the bulky *tert*-butyl group can be removed by using Nafion-H as a catalyst.¹⁷ Following this inspiration, 1,3-diphenylpyrene (3) was successfully synthesized in 85% yield from 7-*tert*-butyl-1,3-diphenylpyrene, which is a key step for building dipolar architectures along the *Z*-axis.¹⁸ The detailed synthetic procedure is illustrated in Scheme 1. Further bromination of 3 afforded 1,3-dibromo-6,8-diphenylpyrene (4) in high yield (79%).¹⁹ Compound 4 is a novel bromide precursor used for synthesizing the desired dipolar architectures (5). This is the first example of the regioselective, stepwise, and asymmetric substitution of pyrene at the active 1,3- and 6,8-positions. Compared with that along the short axis (4-, 5-, 9-, and 10-position) or at 2,7-positions, and introduction of a dipole to pyrene as well, asymmetric functionalization at both 1,3- and

6,8-positions of pyrene shows potential advantages. (a) More artificial dipolar pyrene-based molecules would be synthesized from bromopyrene intermediations than by Pd-catalyzed forms. (b) Introduction of the substitutions at 1,3,6,8-positions would lead to a special influence on both the S₂ ← S₀ and S₁ ← S₀ transition^{18,19} compared with other substitution patterns. (c) This strategy is beneficial for tuning the band gap of the dipolar architectures to realize color control by introducing the substitution groups. For comparison, 1,3,6,8-tetraphenylpyrene (TPPy, 6)²⁰ was synthesized.

Suitable single crystals were obtained by slow evaporation of a CH₂Cl₂/hexane solvent for 2,¹⁶ 5b (CCDC 1025083), and 6 (CCDC 1025084) and a CH₂Cl₂/acetone solvent for 3 (CCDC 1025085) at rt. The crystal structures are presented in Figure 1 and the Supporting Information. Generally, the

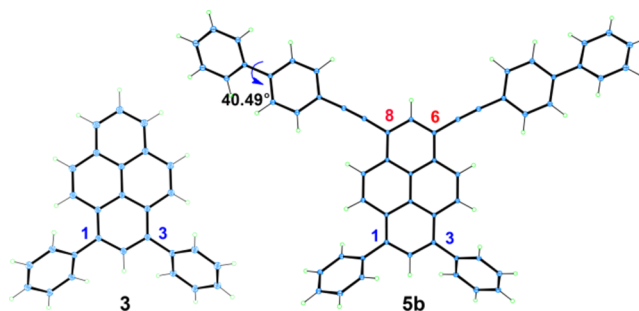


Figure 1. X-ray structures of molecules 3 and 5b.

packing of the structures and the molecular conformation in the crystal were influenced by short intermolecular interactions or the π -stacking present. For instance, the phenyl moieties located at the pyrene 1,3-positions in 2 are all twisted with torsion angles in the range of 45–65° relative to the pyrene plane, which is arranged in a herringbone motif with a slip angle of 28°.¹⁶ Molecules of 3 are held together by strong face-to-face $\pi \cdots \pi$ stacking interactions with a shortest separation of 3.31 Å.

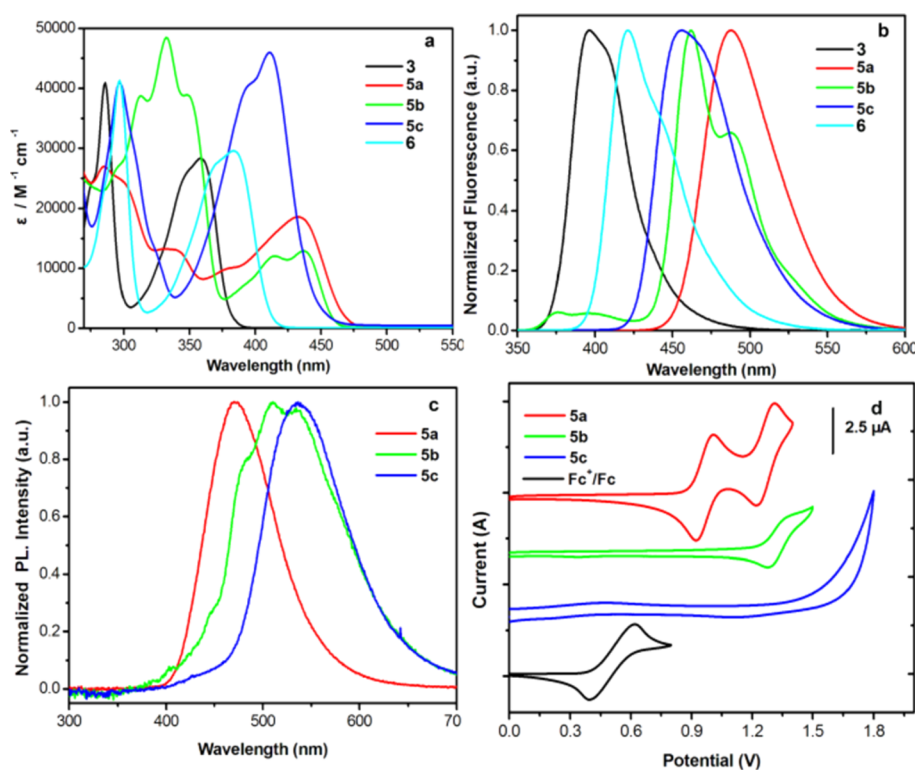


Figure 2. (a) Absorption and (b) fluorescence spectra of 3, 5, and 6 in CH_2Cl_2 . (c) PL spectra and (d) cyclic voltammograms of 5.

Table 1. Photophysical and Electrochemical Properties of Compounds 3, 5, and 6

R	$\lambda_{(S_1 \leftarrow S_0)}^a$ (nm) [ϵ ($\text{M}^{-1} \text{cm}^{-1} \text{L}$)]	$\lambda_{(S_2 \leftarrow S_0)}^a$ (nm) [ϵ ($\text{M}^{-1} \text{cm}^{-1} \text{L}$)]	$\lambda_{\text{max Abs}}^b$ (nm)	$\lambda_{\text{max PL}}$ (nm)	Stokes shift (nm)	Φ_f^c	HOMO ^e (IP) ^d (eV)	LUMO (eV)	energy gap (eV)
3	357 (28000)	286 (41000)	359	396 ^a (462) ^b	39 (103)	0.27 ^a (0.03) ^b	-5.14 (-5.83)	-1.58 ^e (-2.76) ^f	3.56 ^e (3.07) ^g
5a	433 (18500)	285 (27000)	438	488 (469)	55 (31)	0.92 (0.42)	-4.84 (-5.70)	-1.88 (-3.15)	2.97 (2.55)
5b	437 (12900)	332 (48400)	455	462 (510)	25 (55)	0.90 (0.44)	-4.93 (-5.77)	-2.12 (-3.24)	2.80 (2.53)
5c	411 (46100)	296 (41000)	425	456 (537)	45 (112)	0.96 (0.32)	-5.90 (-)	-2.69 (-)	3.21 (2.69)
6	394 (29500)	304 (41200)	400	421 (464)	27 (64)	0.87 (0.52)	-5.01 (-5.76)	-1.69 (-2.93)	3.32 (2.83)

^aMeasured in dichloromethane at room temperature. ^bAs a thin film. ^cDFT/B3LYP/6-31G* using Gaussian. ^dDetermined using AC-3. ^eLUMO = Eg + HOMO. ^fLUMO (eV) = Eg - IP. ^gCalculated from λ_{edge} in a thin film. IP > 6.2 eV.

Dipolar molecule **5b** exhibited a π -stacked packing motif with π - π distances in the range of 3.38–3.51 Å, but no π ... π stacking was observed in **6** (see the Supporting Information). Interestingly, **5b** is remarkably planar with a twist angle of approximately of 40.49(3)° between the adjacent rings of the biphenyl moiety, which is consistent with reported values.²¹ The intriguing conformations of the dipolar molecules can also lead to special optical properties.

The effects on the photophysical properties of a series of 1,3-diphenyl 6,8-donor/acceptor asymmetrically substituted pyrenes **3**, **5**, and **6** are discussed. Figure 2 exhibits the absorption spectra of **3**, **5**, and **6** in dilute dichloromethane. In the D- π -A type molecules, with a strong -NPh₂F donor in **5a**, the absorption spectra exhibited a weak but broad band in the low-energy absorption (375–400 nm), which indicated a charge-transfer (CT) excitation between the donor and acceptor moieties. For **5b**, a broad band around 332 nm is mainly due to a localized π - π^* excitation of the biphenylethynyl group with high extinction coefficients ($\epsilon = 48400 \text{ mol}^{-1} \text{cm}^{-1} \text{L}$). In contrast, the strong -CN acceptor group in **5c** has a strong influence on both the $S_1 \leftarrow S_0$ and $S_2 \leftarrow S_0$ excitations, consistent with the large extinction coefficients with oscillator

strengths. However, compounds **3** and **6** exhibited a similar absorption pattern with little influence on the $S_1 \leftarrow S_0$ or $S_2 \leftarrow S_0$ excitation, as reflected in the similar extinction coefficients (Table 1). Obviously, with an electron-withdrawing group asymmetrically substituted at the 6,8-positions, the $S_1 \leftarrow S_0$ excitation has high extinction coefficients, while the electron donors play a significant role in influencing both the $S_1 \leftarrow S_0$ and $S_2 \leftarrow S_0$ excitations by decreasing the extinction coefficients.

The emission maxima of **3**, **5**, and **6** were in the range of 396–488 nm in dilute dichloromethane solutions with a systematic bathochromic shift following the order $3 < 6 < 5c < 5b < 5a$, suggesting that the energy gap could be fine-tuned between the ground and excited states by choosing the substituent group. The fluorescence of **5a** exhibited pronounced positive solvatochromism with an intramolecular charge-transfer (ICT) state, in which the emission wavelength displays a large red shift from 464 nm (in cyclohexane) to 503 nm (in DMF) (see the Supporting Information), whereas the D- π -A conjugated compound **5b** displayed a maximal emission peak at 462 nm with a shoulder at 488 nm and contributed to an efficient mesomeric intramolecular charge-transfer (MICT)

emission, due to the twist angle [40.49(3)°] of the Franck–Condon vertical state between the diphenyl moieties.²² The spectroscopic and photophysical properties of dipolar molecules **5** exhibit a solvent dependency. The linear relationship of the Stokes shift (ΔV_{st}) versus the solvent parameters (ϵ and n) of **5** was determined by a Lippert–Mataga plot.¹⁶ Obviously, the MICT of the solvent polarity dependence of the fluorescence bands is weaker than for the TICT case (see the Supporting Information).

Compounds **5b** and **5c** as films exhibited green emission and displayed $\lambda_{film,max}$ values of 510 and 537 nm, respectively, which are significantly red-shifted relative to those of their solutions because of the planar structure of the molecule that tends to form dimers. However, the maximum of **5a** was blue-shifted by 19 nm compared with the measurement in solution, because of the presence of the bulky electron donor -NPh₂F moiety that not only plays a role in suppressing aggregation in the solid but also affects the conformation of the electronic structures, therefore, can tune the energy gap. Additionally, in solution, dipolar molecules **5** have similar PL quantum yields (>0.90) in solution, suggesting they display excited state ICT character. The red-shifted emission with decreased quantum yields of **5** (0.32–0.44) in the solid state is attributed to the π – π stacking interactions, whereas **3**, both in solution and in thin films, exhibited the lowest PL efficiencies, which can be attributed to the strong molecular aggregation.

The electrochemical properties of **5** were investigated by cyclic voltammetry (CV). The oxidation of **5a** and **5b** displayed a quasi-reversible oxidation process with HOMO energy levels of –5.15 and –5.51 eV, respectively. For compound **5c**, the oxidation wave was not clearly observed because of the presence of the strongly electron-withdrawing -CN group. The result was further confirmed by photoelectron spectroscopy. The ionization potentials of **3**, **5a**, **5b**, and **6** are measured in a thin film, and their IP values are 5.83, 5.70, 5.77, and 5.76 eV, respectively (Table 1). However, in the presence of the strong electron-withdrawing -CN group in **5c**, the maximal IP range was greater than the instrument full scale (6.2 eV). The optical gaps of **3**, **5**, and **6** were calculated from the absorption spectra of their thin films at 3.07, 2.55, 2.53, 2.69, and 2.83 eV.

The energy gap was further evaluated by density functional theory (DFT) calculations. As shown in Figure 3, obviously, because of the substituents asymmetrically located at the 1,3- and 6,8-positions, the HOMO of **5a** is mainly spread over the -NPh₂F moiety and the pyrene ring, whereas the LUMO extended on the pyrene core and the phenyl rings, which implies a partial charge separation between the donor (-NPh₂F moiety) and acceptor (phenyl moiety). For **5b**, the HOMO and LUMO were delocalized in the pyrene moiety. However, with strong acceptor -CN in **5c**, the HOMO is located over the entire molecular skeleton and the LUMO mostly existed at the pyrene and cyano groups. Obviously, the ICT states would be formed in molecules **5a** and **5c** along the Z-axis with a strong donor at the 1,3-positions and an acceptor at the 6,8-positions. The calculated HOMO–LUMO gap of **5a–c** is 2.97, 2.81, and 3.21 eV, respectively. In addition, the fully optimized structure of **5b** is shown to exhibit a C21–C22–C25–C26 twist angle of 36°, very close to that of the X-ray structure.

CONCLUSION

In summary, a facile synthetic strategy for the construction of dipolar architectures in which the asymmetric unit, including phenyl rings and NPh₂F/biphenylethynyl/CN moieties, is

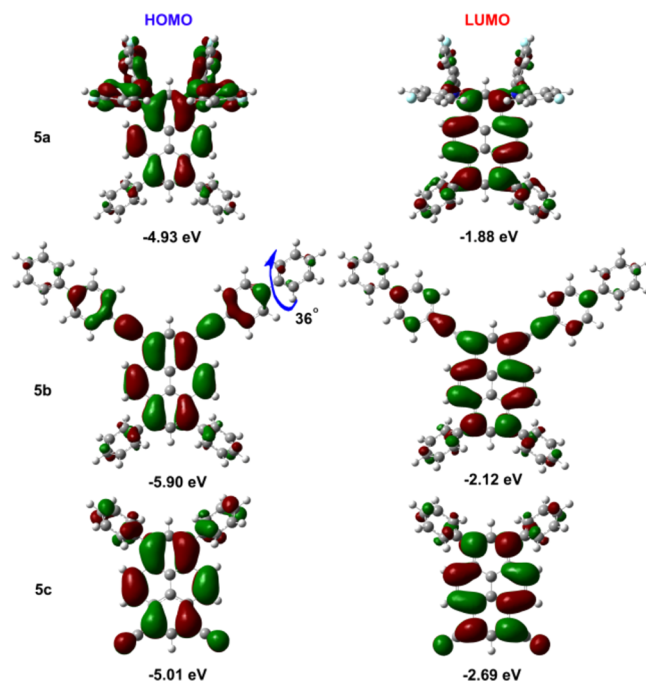


Figure 3. Computed molecular orbital plots (B3LYP/6-31G*) of **5a–c**.

introduced into the 1,3- and 6,8-positions along the Z-axis of the pyrene core by regioselective substitution was explored. X-ray analysis has confirmed the novel asymmetric substitution of the pyrene core. The small dipolar molecule pyrene-based compounds possess a fine ICT state between the donor and acceptor units in the ground state. This article presents a revolutionary methodology for the functionalization of the pyrene core and has potential application in organic photonics.

EXPERIMENTAL SECTION

General. All melting points are uncorrected. ¹H and ¹³C NMR spectra were recorded on a FT-NMR spectrometer (300 and 400 MHz, respectively) and referenced to 7.26 and 77.0 ppm, respectively, for chloroform-*d* solvent with SiMe₄ as an internal reference. *J* values are given in hertz. IR spectra were measured for samples as KBr pellets in a FT-IR spectrophotometer. Mass spectra were obtained with a mass spectrometer at 75 eV using a direct-inlet system. UV/vis spectra were recorded with a UV/vis/NIR spectrometer in various organic solvents. Fluorescence spectroscopic studies were performed in various organic solvents in a semimicro fluorescence cell with a spectrophotometer. Fluorescence quantum yields were measured using absolute methods. Differential scanning calorimetry (DSC) was performed under a nitrogen atmosphere at a heating rate of 10 °C min⁻¹. Photoluminescence spectra were recorded using a luminescence spectrometer. The ionization potential was determined by atmospheric photoelectron spectroscopy. Electrochemical properties of HOMO levels were determined with an electrochemical analyzer. Cyclic voltammetry was performed in 0.10 M tetrabutylammonium perchlorate in anhydrous dichloromethane and THF at a scan rate of 100 mV s⁻¹ at room temperature. The quantum chemistry calculations were performed with the Gaussian 03W (B3LYP/6-31G* basis set) software package. Crystallographic data were collected using graphite monochromated Mo K α radiation ($\lambda = 0.71073$ Å) in the ω scan mode. Data (excluding structure factors) for the structures reported here have been deposited with the Cambridge Crystallographic Data Centre. CCDC 1025083–1025085 contain the supplementary crystallographic data for this paper. These data can be obtained free of charge from The Cambridge Crystallographic Data Centre via www.ccdc.cam.ac.uk/data_request/cif.

Film Preparation. The thin films were prepared by a solution process. A 10 mg sample is dissolved in 1 mL of a toluene solution, and the solution is placed on the substrate, which is then rotated at high speed to spread the fluid by centrifugal force.

Material. Unless otherwise stated, all other reagents used were purchased from commercial sources and were used without further purification. The preparations of 2-*tert*-butylpyrene²³ and 7-*tert*-butyl-1,3-dibromopyrene¹⁶ were described previously.

Synthesis of 7-*tert*-Butyl-1,3-diphenylpyrene (2).¹⁶ A mixture of 7-*tert*-butyl-1,3-dibromopyrene (1) (200 mg, 0.5 mmol), phenylboronic acid (250 mg, 2.0 mmol) in toluene (12 mL), and ethanol (4 mL) at room temperature was stirred under argon, and K₂CO₃ (250 mg, 1.8 mmol) and Pd(PPh₃)₄ (70 mg, 0.06 mmol) were added. After the mixture had been stirred for 30 min at room temperature under argon, the mixture was heated to 90 °C for 24 h while being stirred. After the mixture had been cooled to room temperature, the reaction was quenched with water, and the mixture was extracted with CH₂Cl₂ (2 × 30 mL) and washed with water and brine. The organic extracts were dried with MgSO₄ and evaporated. The residue was purified by column chromatography eluting with a 1:1 CH₂Cl₂/hexane mixture to give 2 as white prisms (1:2 CH₂Cl₂/hexane) (124 mg, 63%): mp 186 °C; IR (KBr) ν_{\max} 2958, 2900, 2866, 1766, 1597, 1484, 1462, 1442, 1396, 1360, 1227, 1151, 875, 837, 810, 764, 702, 613, 503, 457 cm⁻¹; ¹H NMR (300 MHz, CDCl₃) δ 1.59 (s, 9H), 7.44–7.69 (m, 10H), 7.94 (s, 1H), 8.01 (d, *J* = 9.2 Hz, 2H), 8.18 (d, *J* = 9.2 Hz, 2H), 8.20 (s, 2H); ¹³C NMR (75 MHz, CDCl₃) δ 149.23, 141.14, 137.11, 131.16, 130.63, 128.97, 128.35, 127.75, 127.64, 127.22, 125.32, 125.11, 123.42, 122.25, 35.19, 31.89; MS *m/z* 410.2 [M]⁺. Elemental Anal. Calcd for C₃₂H₂₆ (410.2): C, 93.62%; H, 6.38%. Found: C, 93.81%; H, 6.19%.

Synthesis of 1,3-Diphenylpyrene (3). A mixture of 1,3-diphenyl-7-*tert*-butylpyrene (2) (410 mg, 0.09 mmol), Nafion-H (400 mg), and *o*-xylene (4 mL) was refluxed for 24 h and then cooled to room temperature. The solid was removed *in vacuo* and the mother solution collected. The crude product was purified by column chromatography using hexane as an eluent to afford a yellow solid (300 mg, 85%): mp 136.5–137.2 °C; ¹H NMR (300 MHz, CDCl₃) δ 7.45–7.50 (m, 2H), 7.53–7.58 (m, 4H), 7.66–7.68 (m, 4H), 8.00 (d, *J* = 8.8 Hz, 2H), 8.05 (d, *J* = 2.9 Hz, 2H), 8.16 (s, 1H), 8.20 (d, *J* = 2.9 Hz, 2H), 8.22 (s, 1H); ¹³C NMR (100 MHz, CDCl₃) δ 141.01, 137.30, 131.28, 130.65, 129.35, 128.40, 127.93, 127.46, 127.32, 126.13, 125.27, 125.16, 124.98; FABMS *m/z* 354.22 (M⁺). Elemental Anal. Calcd for C₂₈H₁₈ (354.44): C, 94.88%; H, 5.12%. Found: C, 94.85%; H, 5.11%.

Synthesis of 1,3-Dibromo-6,8-diphenylpyrene (4). To a mixture of 1,3-diphenylpyrene 3 (300 mg, 0.85 mmol) in dry CH₂Cl₂ (30 mL) was added dropwise a solution of BTMABr₃ (benzyltrimethylammonium tribromide) (1.0 g, 2.6 mmol) in CH₂Cl₂ (10 mL) and methanol (5 mL) at 0 °C for 1 h under an argon atmosphere. The resulting mixture was allowed to slowly warm to room temperature and stirred overnight. The reaction mixture was poured into ice–water (60 mL) and neutralized with an aqueous 10% Na₂S₂O₃ solution. The mixture solution was extracted with dichloromethane (2 × 20 mL). The organic layer was washed with water (2 × 20 mL) and saturated brine (20 mL), and then the solution was dried (MgSO₄) and condensed under reduced pressure. The crude compound was washed with hot hexane to afford pure 1,3-dibromo-6,8-diphenylpyrene 4 (330 g, 79%) as a yellow solid: mp 184–186 °C; ¹H NMR (400 MHz, CDCl₃) δ 7.49 (m, 2H), 7.53–7.57 (m, 4H), 7.62–7.67 (m, 4H), 8.03 (s, 1H), 8.29 (d, *J* = 9.2 Hz, 2H), 8.33 (d, *J* = 9.6 Hz, 2H), 8.49 (s, 1H); ¹³C NMR (100 MHz, CDCl₃) δ 140.41, 138.61, 133.60, 130.58, 130.47, 129.29, 128.45, 127.91, 127.61, 127.17, 127.10, 125.70, 124.30, 119.24; FABMS *m/z* 510.05 (M⁺). Elemental Anal. Calcd for C₂₈H₁₆Br₂ (512.23): C, 65.65%; H, 3.15%. Found: C, 65.35%; H, 3.34%.

Synthesis of 1,3-Bis[di(4-fluorophenyl)amino]-6,8-diphenylpyrene (5a). The corresponding 1,3-dibromo-6,8-diphenylpyrene (150 mg, 0.29), bis(4-fluorophenyl)amine (180 mg, 0.87 mmol), Pd(OAc)₂ (40 mg, 0.18 mmol), (*t*-Bu)₃P (0.05 mL), sodium *tert*-butoxide (200 mg, 2.05 mmol), and toluene (10 mL) were mixed together and heated at 100 °C for 24 h. The reaction was quenched with water (30 mL) and the organic layer taken into 100 mL of

CH₂Cl₂, washed with a brine solution, and dried over MgSO₄. Evaporation of the solvent under vacuum resulted in a solid residue. The residue was adsorbed on a silica gel and purified by column chromatography using hexane as the eluent and recrystallized from ethyl acetate to afford the corresponding desired compound 5a as a green powder (125 mg, 56%): mp 161.1–162.5 °C; ¹H NMR (400 MHz, CDCl₃) δ 6.84–6.94 (m, 20H), 7.40–7.44 (m, 2H), 7.49 (t, *J* = 7.4 Hz, 8H), 7.53 (s, 1H), 7.56 (d, *J* = 7.2 Hz, 8H), 7.94 (s, 1H), 8.00 (d, *J* = 9.6 Hz, 2H), 8.03 (d, *J* = 9.6 Hz, 2H); ¹³C NMR (100 MHz, CDCl₃) δ 159.27, 156.86, 144.67, 144.65, 141.56, 140.63, 137.89, 130.47, 129.97, 128.48, 128.34, 128.04, 127.40, 126.55, 125.60, 123.19, 123.11, 122.80, 116.07, 115.85; FABMS *m/z* 760.31 (M⁺). Elemental Anal. Calcd for C₅₂H₃₂F₄N₂ (760.82): C, 82.09%; H, 4.24%; N, 3.68%. Found: C, 82.16%; H, 4.39%; N, 3.55%.

Synthesis of 1,3-Bis[3-(biphenyl)ethynyl]-6,8-diphenylpyrene (5b). A mixture of 1,3-dibromo-6,8-diphenylpyrene (50 mg, 0.10 mmol), PdCl₂(PPh₃)₂ (21 mg, 0.03 mmol), CuI (10 mg, 0.05 mmol), PPh₃ (20 mg, 0.08 mmol), and 4-ethynyl-1,1'-biphenyl (53 mg, 0.30 mmol) was added to a degassed solution of triethylamine (5 mL) and *N,N*-dimethylmethanamide (5 mL) under an argon atmosphere. The resulting mixture was stirred at 100 °C for 48 h. After the mixture had cooled to room temperature, the reaction was quenched with water, and the mixture was extracted with CH₂Cl₂ (2 × 30 mL) and washed with water and brine. The organic extracts were dried with MgSO₄ and evaporated. The residue was purified by column chromatography eluting with a 2:1 CH₂Cl₂/hexane mixture to give 5b as a dark yellow powder (1:2 CH₂Cl₂/hexane) (28 mg, 40%): mp 263.1–264.9 °C; ¹H NMR (400 MHz, CDCl₃) δ 7.39 (m, 1H), 7.49 (m, 5H), 7.58 (m, 5H), 7.65–7.71 (m, 13H), 7.77 (d, *J* = 8.2 Hz, 4H), 8.06 (s, 1H), 8.38 (d, *J* = 9.3 Hz, 2H), 8.50 (s, 1H), 8.67 (d, *J* = 9.3 Hz, 2H); ¹³C NMR (100 MHz, CDCl₃) δ 141.92, 141.19, 140.64, 140.31, 140.06, 138.57, 133.31, 132.91, 132.08, 131.98, 130.67, 128.87, 128.41, 128.11, 127.82, 127.66, 127.51, 127.13, 127.07, 127.00, 125.43, 122.22, 120.60, 117.65, 95.38, 88.72; FABMS *m/z* 706.33 (M⁺). Elemental Anal. Calcd for C₅₆H₃₄ (706.87): C, 95.15%; H, 4.85%. Found: C, 95.07%; H, 5.03%.

Synthesis of 1,3-Dicyano-6,8-diphenylpyrene (5c). A mixture of 1,3-dibromo-6,8-diphenylpyrene (2) (100 mg, 0.20 mmol), CuCN (42 mg, 0.49 mmol), and *N*-methyl-2-pyrrolidone (10 mL) was stirred for 24 h and then cooled to room temperature. The solid was removed *in vacuo* and the mother solution collected. Water was added to the solution and the mixture extracted with CH₂Cl₂ (2 × 30 mL) and washed with water and brine. The organic extracts were dried with MgSO₄ and evaporated. The residue was purified by column chromatography eluting with a 4:1 CH₂Cl₂/hexane mixture to give 5c as a yellow powder (43 mg, 54%): mp ≤300 °C; ¹H NMR (400 MHz, CDCl₃) δ 7.56–7.67 (m, 10H), 8.24 (s, 1H), 8.50 (d, *J* = 9.6 Hz, 2H), 8.56 (s, 1H), 8.63 (d, *J* = 8.8 Hz, 2H); ¹³C NMR (100 MHz, CDCl₃) δ 141.95, 139.34, 135.60, 133.55, 131.94, 131.44, 130.71, 128.76, 128.34, 127.41, 124.34, 123.69, 123.58, 117.11, 105.60; FABMS *m/z* 404.35 (M⁺). Elemental Anal. Calcd for C₃₀H₁₄N₂ (404.46): C, 89.09%; H, 3.99%; N, 6.93%. Found: C, 89.19%; H, 3.69%; N, 6.53%.

Synthesis of 1,3,6,8-Tetraphenylpyrene (6).⁹ 1,3,6,8-Tetrabromopyrene (200 mg, 0.386 mmol), phenylboronic acid (254 mg, 2.08 mmol), Pd(PPh₃)₄ (50 mg, 0.04 mmol), and 2.0 M aqueous NaOH (2 mL) were mixed in a flask containing argon-saturated toluene (10 mL). The reaction mixture was stirred at 90 °C for 20 h. After it was cooled to room temperature, the reaction mixture was extracted with dichloromethane (2 × 40 mL). The combined organic extracts were dried with anhydrous MgSO₄ and evaporated. The crude product was purified by column chromatography using a 1:4 hexane/dichloromethane mixture as the eluent to provide a pale powder and recrystallized from hexane to afford 1,3,6,8-tetraphenylpyrene 6 as a light yellow powder (146 mg, 74%): mp 300.1–301.8 °C; IR ν_{\max} (KBr) 2952, 1608, 1513, 1494, 1459, 1286, 1245, 1176, 1106, 1035, 835, 549, 476 cm⁻¹; ¹H NMR (400 MHz, CDCl₃) δ 7.43–7.47 (m, 2H), 7.53 (t, *J* = 7.6 Hz, 8H), 7.66 (d, *J* = 8.0 Hz, 8H), 8.00 (s, 2H), 8.17 (s, 4H); ¹³C NMR (100 MHz, CDCl₃) δ 141.04, 137.22, 130.61, 129.50, 128.31, 128.10, 127.26, 125.91, 125.28; FABMS *m/z* 506.30

(M⁺). Elemental Anal. Calcd for C₄₀H₂₆ (506.63): C, 94.83%; H, 5.17%. Found: C, 94.77%; H, 5.29%.

■ ASSOCIATED CONTENT

Supporting Information

The Supporting Information is available free of charge on the ACS Publications website at DOI: 10.1021/acs.joc.5b02128.

¹H and ¹³C NMR data, complete photophysical and electrochemical data, and theoretical data (PDF)

Crystallographic data (CIF)

Crystallographic data (CIF)

Crystallographic data (CIF)

■ AUTHOR INFORMATION

Corresponding Authors

*E-mail: yamatot@cc.saga-u.ac.jp.

*E-mail: hujianyong@snnu.edu.cn.

Notes

The authors declare no competing financial interest.

■ ACKNOWLEDGMENTS

This work was performed under the Cooperative Research Program of "Network Joint Research Center for Materials and Devices (Institute for Materials Chemistry and Engineering, Kyushu University)". We thank the EPSRC (travel grants to C.R.), The Royal Society of Chemistry, The Scientific Research Foundation for the Returned Overseas Chinese Scholars, the State Education Ministry, and The Scientific Research Common Program of Beijing Municipal Commission of Education (18190115/008) for financial support. The Advanced Light Source is supported by the Director, Office of Science, Office of Basic Energy Sciences, of the U.S. Department of Energy under Contract DE-AC02-05CH11231.

■ REFERENCES

- (1) (a) Duan, L.; Qiao, J.; Sun, Y.; Qiu, Y. *Adv. Mater.* **2011**, *23*, 1137–1144. (b) Kulkarni, A. P.; Kong, X.; Jenekhe, S. *Adv. Funct. Mater.* **2006**, *16*, 1057–1066. (c) Tanaka, H.; Shizu, K.; Nakanotani, H.; Adachi, C. *Chem. Mater.* **2013**, *25*, 3766–3771.
- (2) Amb, C. M.; Chen, S.; Graham, K. R.; Subbiah, J.; Small, C. E.; So, F.; Reynolds, J. R. *J. Am. Chem. Soc.* **2011**, *133*, 10062–10065.
- (3) (a) Wudl, F.; Smith, G.; Hufnagel, E. *J. Chem. Soc. D* **1970**, 1453–1454. (b) Torrance, J. B. *Acc. Chem. Res.* **1979**, *12*, 79–86.
- (4) (a) El-Sayed, A.; Borghetti, P.; Goiri, E.; Rogero, C.; Floreano, L.; Lovat, G.; Mowbray, D. J.; Cabellos, J. L.; Wakayama, Y.; Rubio, A.; Ortega, J. E.; de Oteyza, D. G. *ACS Nano* **2013**, *7*, 6914–6920. (b) Sommer, M.; Huettner, S.; Thelakkat, M. *Adv. Polym. Sci.* **2009**, *228*, 123–153. (c) Szarko, J. M.; Rolczynski, B. S.; Lou, S. J.; Xu, T.; Strzalka, J.; Marks, T. J.; Yu, L.; Chen, L. X. *Adv. Funct. Mater.* **2014**, *24*, 10–26. (d) Chaskar, A.; Chen, H.-F.; Wong, K.-T. *Adv. Mater.* **2011**, *23*, 3876–3895. (e) O'Neill, M.; Kelly, S. M. *Adv. Mater.* **2011**, *23*, 566–584.
- (5) (a) Figueira-Duarte, T. M.; Müllen, K. *Chem. Rev.* **2011**, *111*, 7260–7314. (b) Mateo-Alonso, A. *Chem. Soc. Rev.* **2014**, *43*, 6311–6324.
- (6) Yang, S. W.; Elangovan, A.; Hwang, K. C.; Ho, T. I. *J. Phys. Chem. B* **2005**, *109*, 16628–16635.
- (7) Anthony, J. E. *Chem. Rev.* **2006**, *106*, 5028–5048.
- (8) (a) Elmalem, E.; Biedermann, F.; Johnson, K.; Friend, R. H.; Huck, W. T. S. *J. Am. Chem. Soc.* **2012**, *134*, 17769–17777. (b) Andrade, C. D.; Yanez, C. O.; Rodriguez, L.; Belfield, K. D. *J. Org. Chem.* **2010**, *75*, 3975–3982.
- (9) Feng, X.; Hu, J.-Y.; Iwanaga, F.; Seto, N.; Redshaw, C.; Elsegood, M. R. J.; Yamato, T. *Org. Lett.* **2013**, *15*, 1318–1321.

(10) (a) Lee, Y. O.; Pradhan, T.; No, K.; Kim, J. S. *Tetrahedron* **2012**, *68*, 1704–1711. (b) Oh, H. Y.; Lee, C.; Lee, S. *Org. Electron.* **2009**, *10*, 163–169.

(11) Zöphel, L.; Beckmann, D.; Enkelmann, V.; Chercka, D.; Rieger, R.; Müllen, K. *Chem. Commun.* **2011**, *47*, 6960–6962.

(12) Venkataramana, G.; Dongare, P.; Dawe, L. N.; Thompson, D. W.; Zhao, Y.; Bodwell, G. *Org. Lett.* **2011**, *13*, 2240–2243.

(13) (a) Zöphel, L.; Enkelmann, V.; Müllen, K. *Org. Lett.* **2013**, *15*, 804–807. (b) Keller, S. N.; Veltri, N. L.; Sutherland, T. C. *Org. Lett.* **2013**, *15*, 4798–4801.

(14) (a) More, S.; Bhosale, R.; Choudhary, S.; Mateo-Alonso, A. *Org. Lett.* **2012**, *14*, 4170–4173. (b) Kawano, S.-i.; Baumgarten, M.; Chercka, D.; Enkelmann, V.; Müllen, K. *Chem. Commun.* **2013**, *49*, 5058–5060.

(15) Feng, X.; Iwanaga, F.; Hu, J.-Y.; Tomiyasu, H.; Nakano, M.; Redshaw, C.; Elsegood, M. R. J.; Yamato, T. *Org. Lett.* **2013**, *15*, 3594–3597.

(16) Feng, X.; Hu, J.-Y.; Yi, L.; Seto, N.; Tao, Z.; Redshaw, C.; Elsegood, M. R. J.; Yamato, T. *Chem. - Asian J.* **2012**, *7*, 2854–2863.

(17) Feng, X.; Hu, J.-Y.; Tomiyasu, H.; Seto, N.; Redshaw, C.; Elsegood, M. R. J.; Yamato, T. *Org. Biomol. Chem.* **2013**, *11*, 8366–8374.

(18) Crawford, A. G.; Dwyer, A. D.; Liu, Z.-Q.; Steffen, A.; Beeby, A.; Pålsson, L.-O.; Tozer, D. L.; Marder, T. B. *J. Am. Chem. Soc.* **2011**, *133*, 13349–13362.

(19) Sato, T.; Uejima, M.; Tanaka, K.; Kaji, H.; Adachi, C. *J. Mater. Chem. C* **2015**, *3*, 870–878.

(20) Oyamada, T.; Akiyama, S.; Yahiro, M.; Saigou, M.; Shiro, M.; Sasabe, H.; Adachi, C. *Chem. Phys. Lett.* **2006**, *421*, 295–299.

(21) Low, P. J.; Paterson, M. A.; Yufit, J. D. S.; Howard, J. A. K.; Cherryman, J. C.; Tackley, D. R.; Brook, R.; Brown, B. *J. Mater. Chem.* **2005**, *15*, 2304–2315.

(22) Dekhtyar, M.; Rettig, W.; Weigel, W. *Chem. Phys.* **2008**, *344*, 237–250.

(23) Miura, Y.; Yamano, E.; Tanaka, A.; Yamauchi, J. *J. Org. Chem.* **1994**, *59*, 3294–3300.